JOURNAL OF AGRICULTURAL AND FOOD CHEMISTRY

Article

pubs.acs.org/JAFC

Insight into the Molecular Mechanisms of Propolis Activity using a Subcellular Proteomic Approach

Tanja Petelinc, Tomaž Polak, and Polona Jamnik*

Department of Food Science and Technology, Biotechnical Faculty, University of Ljubljana, Ljubljana SI-1000, Slovenia

ABSTRACT: The effects of a fractionated 70% ethanolic extract of propolis were analyzed at the subproteome level by two-dimensional electrophoresis. Differential detergent fractionation was used to fractionate proteins from the yeast *Saccharomyces cerevisiae* according to their subcellular localization. Thus, four subcellular proteomes were obtained: cytosolic, membrane/organelle, nuclear, and cytoskeletal. Yeast treatment resulted in changes in the levels of proteins involved in carbohydrate and energy metabolism, antioxidant defense, actin filament dynamics, folding of proteins, and others. On the basis of this information, we can obtain better insights into the processes that are carried out in cells exposed to propolis extract.

KEYWORDS: *Two-dimensional electrophoresis, subcellular fractionation, propolis, yeast*

INTRODUCTION

Propolis is a resinous substance that bees collect and use in their hive as a building material and as a disinfectant. In general, it contains resins and balsams (50%), waxes (30%), aromatic and essential oils (10%), pollen (5%), and other organic matter (5%). Because of various potentially beneficial properties of propolis, including antioxidative, anticancer, antibacterial, antiviral, and antifungal effects, it is an intriguing subject of research.[1−7] However, the molecular mechanisms of propolis activities remain largely unknown.

In our previous study, a 70% ethanolic extract of propolis was fractionated using polarity-based solid-phase extraction. Following exposure of the yeast *Saccharomyces cerevisiae* to the propolis fractions obtained, the effects were analyzed at the cellular level. The fraction termed 'eluate EL70' had the greatest effects on the yeast in terms of decreasing intracellular oxidation and increasing cellular metabolic energy.[8]

Yeast *S. cerevisiae* was used as a model organism, which is an excellent model for investigating fundamental cellular processes, stress responses, and metabolic pathways of the human.[9,10] Comparative genomics studies have shown that 40% of yeast proteins share amino acid sequence similarity with at least one human protein[11] and that 30% of genes with a recognized involvement in human disease have an orthologue in yeast.[12] Yeast presents many technical advantages over human cells. It is well-suited to high-throughput methods because its life cycle is rapid, it can grow as dispersed cells in liquid or as colonies on solid media, and its culture requires neither elaborate sterile technique nor expensive media. It is highly amenable to genetic modifications such as gene disruption, deletion, and replacement.[13] Experiments with yeast are easier technically, more rapid, and much less costly than experiments with human cells.[14] The ease of genetics, combined with the ease of growth, makes *S. cerevisiae* a model organism that beautifully combines the power of genetics with that of biochemical studies.[15]

In the present study, the influence of the eluate EL70 fraction (henceforth referred to as EL70) was further analyzed at the proteome level of yeast *S. cerevisiae* using two-dimensional (2D) electrophoresis. Subcellular fractionation was used to reduce the complexity of the protein extracts as well as for the enrichment of low-abundance proteins. These are poorly represented when a classic proteomic approach with a single extraction buffer is applied, thus losing information about important classes of proteins, such as transcriptional factors and regulatory proteins. Furthermore, subcellular fractionation enables an extracted protein to be associated with its localization in the cell, which also correlates strongly with the protein function.

Conventional subcellular fractionation procedures involve differential and density-gradient centrifugation.[16] However, newer techniques use the stepwise fractionation of cellular proteins that is based on the different solubilities of the different cellular compartments in detergents of increasing solubilization efficiency.[17] There are several kits now available for differential detergent fractionation, one of which is the ProteoExtract subcellular proteome extraction kit. This kit is designed for use with mammalian cells, and it yields four subcellular fractions that are enriched in cytosolic, membrane/organelle, nuclear, and cytoskeletal proteins. Previous studies have shown the use of this kit on a variety of cell types, including the SAOS2 osteosarcoma cell line, the A-431 epidermoid carcinoma cell line,[18] human colon mucosa cells,[19] frozen rat liver and heart tissue,[20] and human pancreatic cancer tissue.[21] Here, to the best of our knowledge, we provide the first report of the application of this kit to yeast cells to provide useful insight into our investigations into the molecular mechanisms of propolis activity.

MATERIALS AND METHODS

Chemicals and Standards. The Bradford reagent was from Bio-Rad. Peptone and yeast extract were from Biolife. Ammonium formate was from Fluka. The immobilized pH gradient (IPG) buffer and 3-[(3-

Received: September 19, 2013
Revised: November 6, 2013
Accepted: November 6, 2013
Published: November 6, 2013

cholamidopropyl)dimethylammonio]-1-propanesulfonate (CHAPS) were from GE Healthcare. SYPRO Ruby was from Invitrogen. Ethanol, glucose, hydrochloric acid (HCl), and methanol, were from Merck. Phosphate-buffered saline (PBS) was from Oxoid. Modified porcine trypsin was from Promega. Bovine serum albumin, bromophenol blue, dithiothreitol, glycerol, iodoacetamide, sodium dodecyl sulfate (SDS), thiourea, urea, tris(hydroxymethyl)-aminomethane (Tris), and 4-hydroxy-α-cyano-cinnamic acid were from Sigma.

Sample Preparation. Propolis was collected from a bee hive in the Savinjska Valley (Slovenia) during the autumn of 2010. A propolis sample (10 g) was extracted using 70% ethanol (100 mL) by mixing for 1 h at room temperature. The crude propolis extract was obtained after centrifugation (3000*g*, 5 min) of the extraction mixture and concentration of the supernatant under vacuum using a rotary evaporator.

Solid-Phase Extraction. Solid-phase extraction was used to separate the crude propolis extract into five elution fractions according to polarity. The crude propolis extract (200 μL) was mixed with 20 mM ammonium formate, pH 3.2 (200 μL), and then added onto a STRATA-X solid-phase extraction cartridge containing 33 μm polymeric reverse-phase sorbent (60 mg/3 mL tube; catalog no. 8B-S100-UBJ; Phenomenex) that had previously been conditioned with methanol (2 mL) and equilibrated with 20 mM ammonium formate, pH 3.2 (2 mL). After the loading of the sample, the cartridge was washed with 20 mM ammonium formate in 15% methanol (2 mL) and vacuum-dried for 3 min. Next, the cartridge was eluted with 30% ethanol (2 mL) followed by 40% ethanol (2 mL), 50% ethanol (2 mL), 60% ethanol (2 mL), and 70% ethanol (2 mL). This provided the propolis fractions as the 30 (EL30) to 70% (EL70) ethanol eluates.

In the present study, EL70 was used. The composition of EL70 was determined in our previous study using liquid chromatography–tandem mass spectrometry, and the total phenolic content was determined using the Folin–Ciocalteu method (0.83 g of galic acid equivalent/L).[8]

Yeast Strain and Cultivation. The ZIM 2155 *S. cerevisiae* strain was obtained from the Culture Collection of Industrial Microorganisms (ZIM) of the Biotechnical Faculty, University of Ljubljana, Ljubljana, Slovenia.

The yeast cells were cultivated in yeast extract (10 g/L), peptone (20 g/L), and glucose (20 g/L) (YEPD) medium at 28 °C and with agitation at 220 rpm on a rotary shaker until they reached the stationary phase. The cells were then centrifuged (4000*g*, 3 min), washed once with PBS, and resuspended in PBS at 1×10^8 cells/mL. The yeast cells were further incubated at 28 °C and 220 rpm for 96 h.

Yeast Treatment. Following the 96 h incubation in PBS, the yeast cells were treated with EL70 (1% v/v). After a further 2 h incubation at 28 °C and 220 rpm, the yeast samples from three biological replicates were used for protein analysis.

Extraction of Subcellular Proteomes. Yeast suspensions (20 mL) were centrifuged (4000*g*, 3 min). The cell pellet obtained was washed twice with PBS and frozen at −80 °C until the extraction of the subcellular proteomes using the ProteoExtract subcellular proteome extraction kit (Calbiochem).

This kit was used according to manufacturer's instructions with some modifications. Briefly, the thawed yeast cell pellet was washed twice with wash buffer. After centrifugation (300*g*, 10 min, 4 °C), 1 mL of the first extraction buffer (containing 5 μL of protease inhibitor cocktail) was added to the cell pellet. The cells were disrupted with zirconia/silica beads (BioSpec Products) by vortexing five times for 1 min each spaced with 1 min intervals for cooling on ice. The supernatant obtained following centrifugation (1000*g*, 10 min, 4 °C) was stored as fraction 1 (F1), and the pellet was washed three times with 1 mL of the first extraction buffer. Then, following a 30 min incubation of the pellet with 1 mL of the second extraction buffer (containing 5 μL of protease inhibitor cocktail) with gentle agitation, fraction 2 (F2) was recovered by centrifugation (6000*g*, 10 min, 4 °C). The pellet obtained was washed two times with 1 mL of the second extraction buffer. Next, 0.5 mL of the third extraction buffer (containing 5 μL of protease inhibitor cocktail and 1.5 μL of the Benzonase nuclease) was added to the pellet. After a 10 min incubation with gentle agitation, the supernatant following centrifugation (7000*g*, 10 min, 4 °C) was stored as fraction 3 (F3), and the pellet was washed once with 0.5 mL of the third extraction buffer. Finally, fraction 4 (F4) was obtained following addition of 0.5 mL of the final extraction buffer (containing 5 μL of protease inhibitor cocktail) to the pellet and resuspension of the sample by pipetting.

The protein concentration in each of the fractions was determined according to the method of Bradford,[22] with bovine serum albumin as the standard.

Clean-up of the Fractions. Fractions F2–F4 included a cleanup step prior to 2D electrophoresis because of the low protein concentrations in these samples. Thus, 2D clean-up kits (GE Healthcare) were used. In short and according to the manufacturer's instructions, the volume of the samples that corresponded to 100 μg of protein were mixed with three volumes of the precipitant and incubated on ice for 15 min. Afterward, three volumes of the coprecipitant was added followed by centrifugation (8000*g*, 10 min, 4 °C). More of the coprecipitant (80 μL) was added to the pellet, and once it was resuspended, it was incubated on ice for 5 min. After centrifugation (8000*g*, 5 min, 4 °C), double-distilled water (50 μL), chilled wash buffer (1 mL), and the wash additive (5 μL) were added to the pellet, which was then mixed and incubated (30 min, −20 °C), with vortexing every 10 min. Following centrifugation (10 000*g*, 10 min, 4 °C), the pellet was left to air-dry for 5 min and then redissolved in 250 μL of rehydration solution (7 M urea, 2 M thiourea, 2% (w/v) CHAPS, 2% (v/v) IPG buffer (pH 4–7), 18 mM dithiothreitol, and a trace of bromophenol blue) and incubated for 60 min at room temperature, with protein concentrations determined according to the method of Bradford.[22]

Two-Dimensional Electrophoresis. Two-dimensional electrophoresis was performed according to the method of Görg,[23] with minor modifications. The samples (50 μg of protein) were mixed with the rehydration solution (see above) and applied to 13 cm pH 4–7 IPG strips (GE Healthcare). After rehydration, the first dimension of the isoelectric focusing was carried out at 20 °C on a Multiphore II system (GE Healthcare). The following voltage program was applied: 0–300 V as a gradient over 1 min, 300 V fixed for 1 h, 300–3500 V as a gradient over 1.5 h, and 3500 V fixed for 5 h. Prior to the second dimension of the 2D electrophoresis, the IPG strips were equilibrated for 15 min in SDS equilibration buffer (75 mM Tris-HCl (pH 8.8), 6 M urea, 30% (v/v) glycerol, 2% (w/v) SDS, and a trace of bromophenol blue) containing 1% (w/v) dithiothreitol and then for an additional 15 min with the addition of 4.8% (w/v) iodoacetamide. The second dimension (SDS polyacrilamide gel electrophoresis) was carried out with 12% running gels on a vertical SE 600 discontinuous electrophoretic system (Hoefer Scientific Instruments) at a constant 20 mA/gel for 15 min and then at a constant 40 mA/gel until the bromophenol blue reached the bottom of the gel. The 2D gels were stained with SYPRO Ruby.

For each fraction, three 2D gels were run under the same conditions.

Protein Visualization and Image Analysis. After staining, the gels were documented using the CAM-GX-CHEMI HR system (Syngene). This gel image analysis was carried out using the 2D Dymension software, version 2.02 (Syngene). The 2D gels of the particular fractions extracted from the treated yeast were compared to the gels of the corresponding fraction from the control cells.

The spots on the gels were quantified on the basis of their normalized volumes as the spot volume divided by the total volume of all of the spots resolved in the gels. The expression changes (as fold changes) were considered significant if the intensity of the particular spot reproducibly differed by >1.5-fold between the control and the treated samples and if this was statistically significant (ANOVA).

Protein Identification and Bioinformatics Analysis. The proteins in the individual spots from the gels were identified using matrix-assisted laser desorption/ionization–time-of-flight/time-of-flight mass spectrometry, at the Proteomics Technology Facility, Department of Biology, University of York (York, United Kingdom), as previously described.[24]

Briefly, a volume of 10 μL of solution containing 0.02 μg/μL of modified trypsin was added to washed and dried gel pieces. Digestion was performed overnight at 37 °C. One microliter of each sample was loaded on a MALDI target plate followed by an equal volume of matrix solution (5 mg/mL of 4-hydroxy-α-cyano-cinnamic acid in 50% (v/v) aqueous acetonitrile containing 0.1% (v/v) trifluoroacetic acid). Positive-ion MALDI mass spectra were obtained using a Ultraflex III MALDI-TOF/TOF (Bruker). The mass spectrometer was externally calibrated with a mixture of des-Arg-Bradykinin, Angiotensin I, Glu-Fibrinopeptide B, ACTH (1-17 clip), ACTH (18-39 clip), ACTH (7-38 clip). The ten strongest peaks of interest were chosen for further MS/MS fragmentation in LIFT mode. FlexAnalysis software (Bruker, version 3.3) was used to perform the spectral processing and peak list generation for both the MS and MS/MS spectra.

Tandem mass spectral data were submitted to database searching using the Mascot program (Matrix Science Ltd., version 2.3) through the ProteinScape interface (Bruker, version 2.1). Spectra were searched against the NCBInr 20101130 database. The following search criteria were applied: *S. cerevisiae* as the species and tryptic digestion with a maximum number of one missed cleavage. The peptide mass tolerance was set to ±100 ppm, and the fragment mass tolerance was set to ±0.5 Da. Additionally, carbamidomethylation and oxidation were considered as possible fixed and variable modifications, respectively. The results were filtered to accept only peptide matches with an expect score of 0.05 or better.

To obtain information about the cellular localization of the proteins identified, the UniProt database was used (http://www.uniprot.org/).

RESULTS AND DISCUSSION

In the present study, the effects of a fractionated 70% ethanolic extract of propolis were studied at the proteome level using 2D electrophoresis as a continuation of our previous study[8] where these activities were investigated primarily at the cellular level.

In classic proteomic procedures, a single buffer is used to extract the cellular proteins. Here, in contrast, the fractionation method was based on the different solubilities of the cellular compartments using sequentially added detergent-containing buffers of increasing extraction efficiency. Thus, we reduced the complexity of the extract as well as enriched the low-abundance proteins, which can otherwise be masked by the high-abundance proteins. The commercially available kit used for the differential detergent fractionation allowed the fractionation of the proteins according to their cellular localization, thus providing four subproteomes. According to the manufacturer, the fractions obtained can be defined as cytosolic (F1), membrane/organelle (F2), nuclear (F3), and cytoskeletal (F4). Because this differential detergent fractionation kit was designed for mammalian cells, we modified the procedure for yeast cells. Thus, two additional steps were added: (1) mechanical cell disruption using zirconia/silica beads and (2) pellet washing between the sequential additions of the different detergent-containing buffers to avoid contamination with proteins from the other subcellular compartments; the numbers of washing steps were determined according to the protein concentrations in the eluates (Figure 1). In addition, prior to 2D gel electrophoresis, F2–F4 were purified and concentrated using a 2D clean-up kit.

Analysis of Subproteomic Profiles. Because the application of this differential detergent fractionation kit to protein extraction from yeast is novel, we first examined whether the protein extraction occurred according to distinct subcellular compartments. Thus, characterization of the four subcellular fractions obtained was carried out.

Analysis of these individual subproteomic profiles separated on the 2D gels showed distinct protein patterns for each

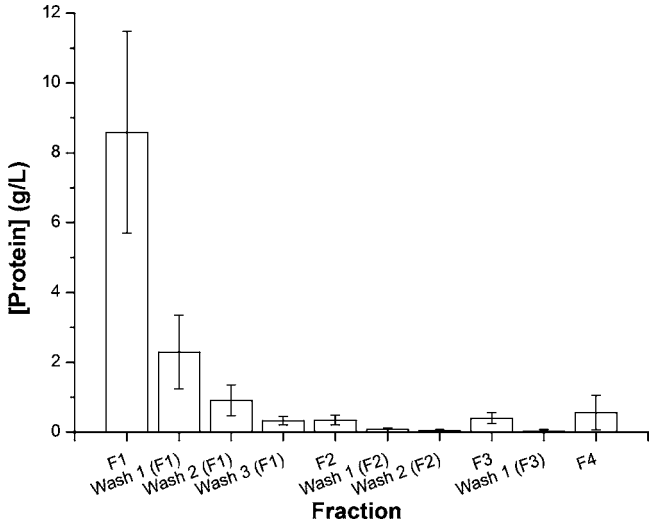

Figure 1. Protein concentrations in the F1–F4 fractions extracted from the yeast *S. cerevisiae* using the subcellular proteome extraction kit.

fraction. Furthermore, some of the protein spots were found only in a single subproteome (Table 1), and as such, they can be used to match each fraction with its specific subcellular compartment. Protein identification and further bioinformatics analysis of the cellular localizations were carried out. As shown in Table 1, the different tentative cellular localizations for the protein spots from each of the single subproteomes were annotated, which also demonstrated that some of the proteins resided in more than one location in the cell.[25] However, this might indicate that a protein shuttles between different compartments to carry out a specific function.[26] On this basis, we evaluated the distributions of the annotations for the cellular localizations of protein spots found in a single, distinct subproteome (Figure 2). Proteins from F2 were annotated to the mitochondrial outer and inner membranes as well as the mitochondrial intermembrane space, whereas the proteins in F3 can be tentatively located to the mitochondrial matrix, mitochondrial nucleoid, and mitochondrial inner membrane. Furthermore, proteins from F3 were also annotated as being of nuclear and chromosomal origins.

By further analyzing the 2D gels, most of the protein spots were found as consensus spots in two or more subproteomic profiles. This might mean that a protein is found in multiple cell locations simultaneously, or it might result from contamination with the proteins from the other subcellular compartments. Proteins can perform different functions depending on their local environment, pH, cofactor availability, protein interactions, and post-translational modifications, such as phosphorylation and proteolysis.[27] Thus, in the case of proteins with multiple locations in the cell, each might imply a different function of the protein. Furthermore, simultaneous fractionation of the cellular proteins according to the subcellular compartments also allowed us to observe dynamic changes in the distribution of these proteins. This is important because proteins can be redistributed in response to a variety of physiological stimuli. Furthermore, activation of numerous cellular regulatory pathways is accompanied by the translocation of key proteins from one subcellular compartment to another.[28] A contamination could be the result of incomplete extraction in the previous step of the extraction procedure, which is important to consider in the case of high-abundance

Table 1. Proteins Expressed in the Single F2 and F3 Subproteomes That Were Extracted from the Yeast *S. cerevisiae* using the Subcellular Proteome Extraction Kit

spot no.	UniProt accession no.	gene name	protein name	theoretical M_r (kDa)/pI	score	matched peptide	sequence coverage (%)	tentative subcellular localization annoted in the UniProt database
F2								
1	P00830	Atp2	ATP synthase subunit beta, mitochondrial	54.8/5.52	666	7(7)	18	Mitochondrion. Mitochondrial inner membrane. Mitochondrial intermembrane space. Cytosol.
2								
3					800	8(8)	21	
					843	8(8)	21	
4	P23644	Tom40	Mitochondrial import receptor subunit TOM40	42.2/5.34	470	5(5)	23	Mitochondrion. Mitochondrial outer membrane. Mitochondrial intermembrane space. Cytosol.
5	P07257	Qcr2	Cytochrome b-c1 complex subunit 2, mitochondrial	40.5/7.67	527	7(7)	23	Mitochondrion. Mitochondrial inner membrane.
6	P08067	Rip1	Cytochrome b-c1 complex subunit Rieske, mitochondrial	23.6/8.24	181	2(2)	13	Mitochondrion. Mitochondrial inner membrane.
7	P00128	Qcr7	Cytochrome b-c1 complex subunit 7	14.6/5.62	379	5(5)	38	Mitochondrion. Mitochondrial inner membrane.
F3								
8	P15705	Sti1	Heat shock protein STI1	66.4/5.45	935	10(10)	21	Cytoplasm.
9					893	10(10)	19	
10					896	10(10)	21	
11	P04147	Pab1	Polyadenylate-binding protein, cytoplasmic and nuclear	64.5/5.71	470	6(6)	12	Nucleus. Cytoplasm. Ribosome. Cytoplasmic stress granule.
12	P16451	Pdx1	Pyruvate dehydrogenase complex protein X component, mitochondrial	45.5/5.55	540	6(6)	22	Mitochondrion. Mitochondrial matrix.
13	P21827	Srm1	Guanine nucleotide exchange factor SRM1	53.5/5.71	112	2(2)	2	Chromosome. Nucleus.
14	P16387	Pda1	Pyruvate dehydrogenase E1 component subunit alpha, mitochondrial	46.7/8.29	186	3(3)	7	Mitochondrion. Mitochondrial matrix. Mitochondrial nucleoid.
15	P07256	Cor1	Cytochrome b-c1 complex subunit 1, mitochondrial	50.3/6.77	317	4(4)	11	Mitochondrion. Mitochondrial inner membrane.
16	P32473	Pdb1	Pyruvate dehydrogenase E1 component subunit beta, mitochondrial	40.1/5.23	649	6(6)	23	Mitochondrion. Mitochondrial matrix. Mitochondrial nucleoid.
17					614	6(6)	23	
18	P53228	Nqm1	Transaldolase NQM1	37.3/5.99	330	5(5)	16	Cytoplasm. Nucleus.
19					355	5(5)	17	

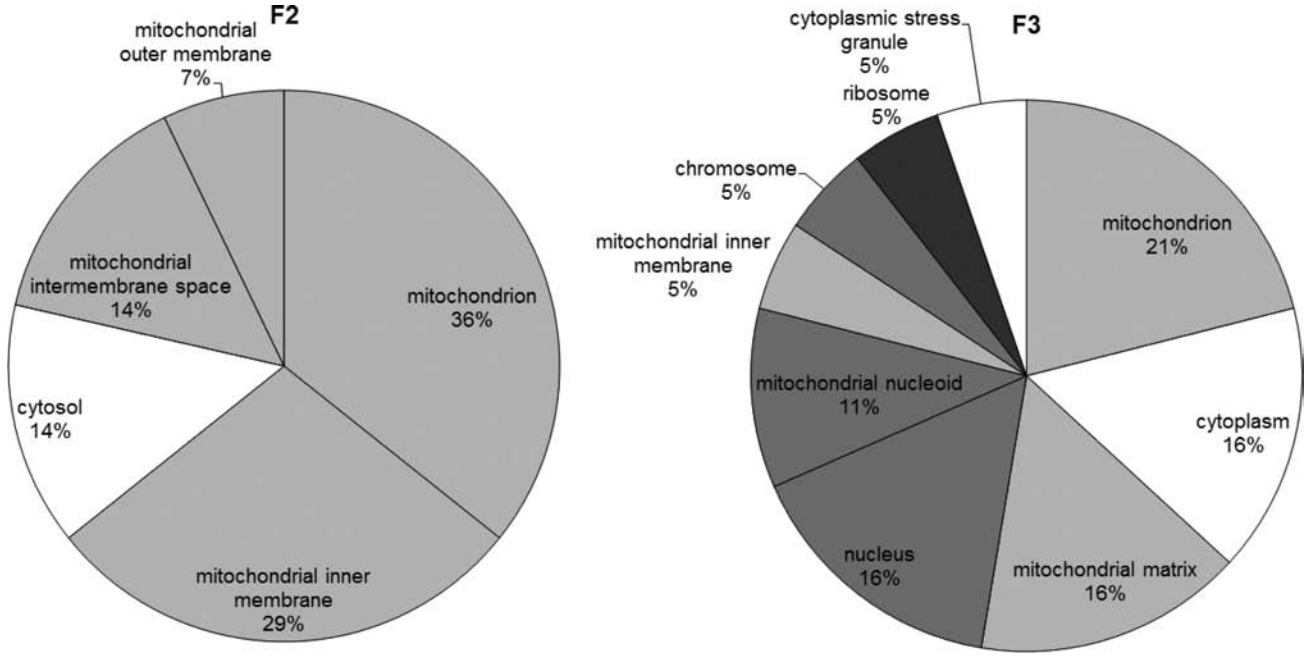

Figure 2. Tentative subcellular localization of the proteins identified that were extracted in a single subproteome, F2 or F3, on the basis of gene ontology annotations.

proteins because these can be present in abundance over the low-abundance proteins by up to 6 orders of magnitude . Even after several washing steps, the quantity of the residue protein might still be high in relation to the low-abundance proteins

dx.doi.org/10.1021/jf4042003 | J. Agric. Food Chem. 2013, 61, 11502−11510

Table 2. Differentially Expressed Proteins in Subproteomes F1, F2, and F4 Extracted from the Yeast *S. cerevisiae* using the Subcellular Proteome Extraction Kit[a]

spot no.	UniProt accession no.	gene name	protein name	fold change (treated vs control)	P value (ANOVA)	theoretical M_r (kDa)/p*I*	score	matched peptide	sequence coverage (%)	tentative subcellular localizations annoted in the UniProt database
F1										
20	P00360	Tdh1	Glyceraldehyde-3-phosphate dehydrogenase 1	−2.9	0.004	43.4/5.30	311	5(5)	13	Cytoplasm. Mitochondrion. Lipid particle. Plasma membrane. Cell wall.
21	P60010	Act1	Actin	−1.8	0.06	41.9/5.44	538	6(6)	23	Nucleus. Cytoskeleton. Chromosome. Cytoplasm.
22	P43616	Dug1	Cys-Gly metallodipeptidase DUG1	−1.5	0.03	53.1/5.43	492	6(6)	17	Cytoplasm. Mitochondrion. Ribosome.
23	P14540	Fba1	Fructose-bisphosphate aldolase	−1.5	0.03	39.9/5.51	510	5(5)	23	Cytoplasm. Mitochondrion. Cytosol.
24	P12709	Pgi1	Glucose-6-phosphate isomerase			61.3/6.00	189	3 (3)	5	Cytoplasm. Mitochondrion. Plasma membrane.
F2										
25	P32381	Arp2	Actin-related protein 2	1.7	0.04	44.2/5.54	171	2(2)	5	Cytoplasm. Mitochondrion. Cytoskeleton.
26	P53312	Lsc2	Succinyl-CoA ligase [ADP-forming] subunit beta, mitochondrial	1.7	0.05	47.2/7.09	270	3 (3)	8	Mitochondrion.
27	Q03558	Oye2	NADPH dehydrogenase 2	1.6	0.04	44.9/6.13	151	3(3)	8	Nucleus. Cytoplasm. Mitochondrion.
28	P07257	Qcr2	Cytochrome b-c1 complex subunit 2, mitochondrial	1.5	0.06	40.5/7.67	784	9(9)	31	Mitochondrion. Mitochondrial inner membrane.
F4										
29	P32835	Gsp1	GTP-binding nuclear protein GSP1/CNR1	−2.2	0.01	25.0/6.11	140	2(2)	8	Cytoplasm. Nucleus.
30	P60010	Act1	Actin	−1.9	0.01	41.9/5.44	538	6(6)	23	Nucleus. Cytoskeleton. Chromosome. Cytoplasm.
31	P06169	Pdc1	Pyruvate decarboxylase isozyme 1	−1.7	0.02	61.7/5.80	211	3(3)	7	Nucleus. Cytoplasm. Cytosol.
32	P14540	Fba1	Fructose-bisphosphate aldolase	−1.7	0.03	39.9/5.51	510	5(5)	23	Cytoplasm. Mitochondrion. Cytosol.
33	P14540			−1.6	0.02		616	6(6)	26	
34	P32473	Pdb1	Pyruvate dehydrogenase E1 component subunit beta, mitochondrial	2.1	0.03	40.1/5.23	328	4(4)	14	Mitochondrion. Mitochondrial matrix. Mitochondrial nucleoid.
35	P07283	Sec53	Phosphomannomutase	2.0	0.002	29.2/5.14	283	3(3)	16	Cytoplasm. Cytosol.
36	P00830	Atp2	ATP synthase subunit beta, mitochondrial	1.6	0.01	54.8/5.52	530	7(7)	18	Mitochondrion. Mitochondrial inner membrane. Mitochondrial intermembrane space. Cytosol.
37	P15992	Hsp26	Heat shock protein 26	1.5	0.01	23.9/5.31	375	4(4)	28	Nucleus. Cytoplasm.

[a]After a 2 h exposure to the bioactive fraction of the 70% ethanolic extract of propolis, EL70 (1% v/v).

dx.doi.org/10.1021/jf4042003 | J. Agric. Food Chem. 2013, 61, 11502−11510

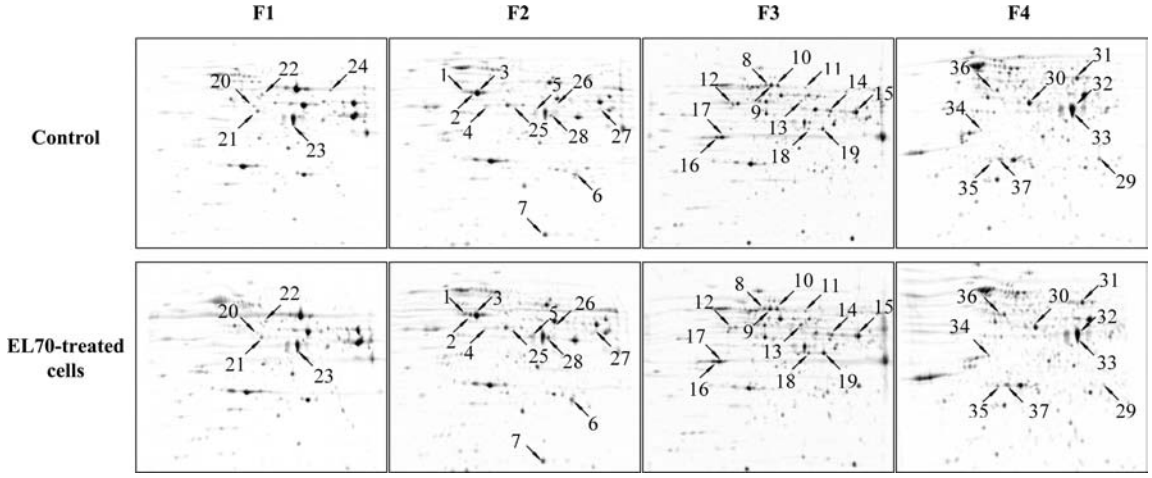

Figure 3. Representative 2D gel images of the four subcellular proteomes extracted from the yeast *S. cerevisiae*, with marked spots for the proteins extracted in a single fraction (1−19) and for the differentially expressed proteins (20−37). Details of the indicated spots are listed in Tables 1 and 2.

extracted in the following step of the procedure. The discrimination between a genuine resident of an enriched cellular compartment or a contaminant is possible by quantification of the consensus protein spots.[25]

Overall, this differential detergent fractionation kit proved to be more suitable for the enrichment of low-abundance proteins from particular cellular compartments rather than to extract the pure subproteomes, which is consistent with previous reports.[18−20]

Propolis Effects on the Yeast Subproteomes. After characterizing these subproteomic profiles, the effects of the EL70 fraction, obtained from the 70% ethanolic propolis extract (Materials and Methods), on these yeast cells was investigated at the proteome level. EL70 is the most active fraction of this 70% ethanolic propolis extract with respect to our previously defined EL70-induced decreases in intracellular oxidation and increases in cellular metabolic energy.[8] Here, a further proteomic study was carried out to understand the activity of EL70 in the cell better and thus to define further the molecular mechanisms of propolis activity.

Recently, propolis effects on yeast cells were examined at the mRNA level.[29,30] However, it should be noted that the abundance of specific mRNAs does not necessarily correlate with the abundance of the corresponding proteins. Therefore, functional changes in cells are best determined by monitoring the proteins that carry out these activities.[28] There was also a study in which the influence of propolis was investigated at the proteome level in cancer cell lines.[31] Differentially expressed proteins were found between the control and treated samples; however, protein identification was not carried out. In the present study, a subproteomic approach was used to study simultaneously the effects of this propolis extract fraction, EL70, on the four fractions extracted from the different cellular compartments by the differential detergent fractionation kit. These protein profiles were compared between the control and the treated samples within the same fraction (e.g., F1 control vs F1 treated). The differentially expressed proteins are summarized in Table 2 and illustrated in Figure 3.

Eighteen proteins showed different levels in the comparisons between the control and treated cells, and these are involved in different cellular processes. Among these, proteins involved in carbohydrate and energy metabolism were the most abundant group (44.4%). The proteins GAPDH (spot 20), FBPA (spot 23), Pgi1p (spot 24), and Pdc1p (spot 31) showed reduced levels upon EL70 treatment, whereas the proteins Lsc2p (spot 26), Qcr2p (spot 28), Pdb1p (spot 34), and Atp2p (spot 36) had increased levels. The second most represented group included proteins associated with actin filament dynamics (22.2%), where Act1p (spot 30) and FBPA (spots 32 and 33) had reduced levels upon EL70 treatment, whereas Arp2p (spot 25) and Hsp26p (spot 37) had increased levels. The proteins identified were also related to oxidative stress responses (11.1%), where Dug1p (spot 22) had decreased levels upon EL70 treatment and Oye2p (spot 27) had increased levels. The proteins Hsp26p (spot 37) and Sec53p (spot 35) had increased levels upon EL70 treatment and are associated with protein folding (11.1%) (Figure 4).

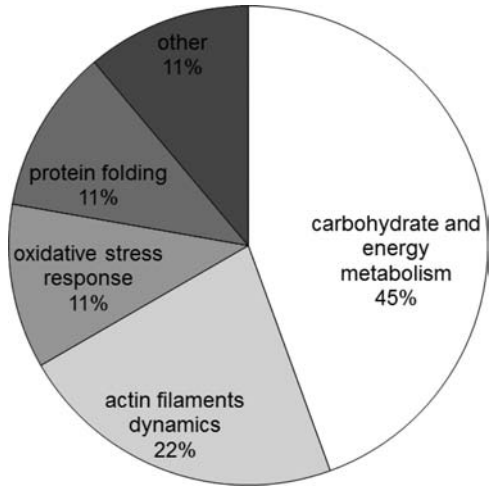

Figure 4. Cellular processes associated with the differentially expressed proteins in the yeast cells treated with EL70 (1% v/v).

In the framework of carbohydrate and energy metabolism, EL70 caused changes in the levels of proteins involved in glycolysis, the tricarboxylic acid cycle, and the mitochondrial respiratory chain. Glyceraldehyde-3-phosphate dehydrogenase 1 (GAPDH) is a key glycolytic enzyme, and it was reduced in the EL70-treated cells. As reported previously, inactivation of GAPDH causes the rerouting of the carbohydrate flux from glycolysis to the pentose phosphate pathway, thus supplying the

cell with NADPH (i.e., providing a reducing equivalent for antioxidant systems).[32] Additionally, we also observed reduced levels of two more glycolytic enzymes: fructose-bisphosphate aldolase (FBPA) and glucose-6-phosphate isomerase. This might indicate the induction of the pentose phosphate pathway in the EL70-treated cells. At the same time, exposure of these cells to EL70 promoted increased levels of pyruvate dehydrogenase E1 component subunit beta (mitochondrial). Pyruvate dehydrogenase converts pyruvate to acetyl-CoA, a substrate for the tricarboxylic acid cycle. In agreement with this, an enzyme that converts pyruvate to acetaldehyde, pyruvate decarboxylase isoenzyme 1, was reduced in these EL70-exposed cells. Furthermore, increased levels were also found for (1) succinyl-CoA [ADP forming] subunit beta (mitochondrial), which is the only enzyme in the tricarboxylic acid cycle that directly produces ATP, (2) cytochrome b-c_1 complex subunit 2 (mitochondrial), which is part of the electron transport chain where the proton motive force is generated, and (3) ATP synthase subunit beta (mitochondrial), which generates ATP in the presence of the proton motive force. These data could explain the increased cellular metabolic energy in yeast treated with EL70 that was shown in our previous study.[8]

The oxidative stress response was also a target of this treatment with EL70, as there were changes in the levels of two proteins associated with antioxidant systems. Exposure of these cells to EL70 promoted reduced levels of the Cys−Gly metallodipeptidase DUG1, which is involved in *S. cerevisiae* degradation of glutathione and which has homologues in bacteria, fungi, plants, and mammals.[33,34] Glutathione degradation has a major impact on the intracellular glutathione concentration, as blocked degradation of glutathione results in an increase in the cellular glutathione content.[35] Therefore, reduced Dug1p can help to maintain the levels of glutathione, an important cellular redox buffer that is involved in responses to sulfur and nitrogen starvation, detoxification of endogenous toxic metabolites and xenobiotics, protection against oxidative stress, and resistance to heavy-metal stress.[36] Moreover, there were increased levels of NADPH dehydrogenase 2 (Oye2p) in cells treated with EL70. An antioxidative role of Oye2p was shown in a study by Odat et al.[37] where the level of reactive-oxygen species (ROS) in cells with overexpressed Oye2p was lower (13%) compared to wild-type cells. Furthermore, NADPH generated in the pentose phosphate pathway can be used by Oye2p[37] or NADPH-dependent glutathione reductase, which maintains the balance between the oxidized and reduced forms of glutathione.[36] Oxidative stress response was expected because enhanced cellular metabolic energy is frequently accompanied by induction of the cellular antioxidant machinery to cope with the increased levels of ROS that are produced during mitochondrial respiration.[37] Thus, decreased levels of Dug1p and increased levels of Oye2p might explain the decreased intracellular oxidation in cells treated with EL70, as reported in our previous study.[8]

Another cellular process that is associated with several differentially expressed proteins is actin filament dynamics. In addition to actin (Act1p) itself, three actin-binding proteins were affected by treatment with EL70: actin-related protein 2 (Arp2p), FBPA, and heat shock protein 26 (Hsp26p). In the case of actin (Act1p), reduced levels were observed in two of the fractions: the cytosolic (F1) and cytoskeletal (F4) fractions. Arp2p is a part of the Arp2/3 complex that promotes actin filament assembly through its capping, nucleating, and branching activity;[38] here, Arp2p had increased levels with the EL70 treatment. Similarly, FBPA is mainly known as a glycolytic enzyme, although it also has a role in the inhibition of actin polymerization;[39] here, FBPA was also decreased in F1 and F4. Finally, for Hsp26p, there were increased levels upon EL70 treatment. Small heat shock proteins (sHSPs) with molecular masses of 15−30 kDa show affinity for actin as well, where it has been shown that the interaction between actin and nonphosphorylated sHSPs inhibits actin polymerization.[40] However, it appears that the binding of phosphorylated sHSPs with actin prevents actin depolymerization.[41] Additionally, Hsp26p might have a role not only in actin dynamics but also as a molecular chaperone that is responsible for correct protein folding under stress conditions.[42] Because the actin cytoskeleton is an early target of ROS,[43] these changes in the levels of actin and actin-binding proteins can be expected.

Other cellular processes were also impacted by EL70 treatment of these yeast. For example, phosphomannose, which catalyzes the conversion of mannose 6-phosphate to mannose 1-phosphate, had increased levels upon EL70 treatment. Together with GTP, mannose 1-phosphate forms GDP-mannose, which is required for the folding and glycosylation of secretory proteins in the lumen of the endoplasmic reticulum.[44] Additionally, reduced levels of the Ran GTPase GSP1/CNR1 were seen. It has been reported that there are increased levels of Ran GTPase in cancer cells.[45,46] Furthermore, it appears that only low levels of Ran GTPase are required for normal cell viability, whereas excessive Ran GTPase activity can deregulate normal cell function, predisposing the cells to tumorigenesis.[47] Thus, the reduced levels of GSP1/CNR1 found in the EL70-treated cells might indicate an antitumor activity of EL70.

On the basis of the information relating to the protein levels and their identities, subcellular localization, and functions, we can obtain better insight into the processes that are carried out in cells exposed to EL70, which results in decreased intracellular oxidation and increased cellular metabolic energy, as was also described in our previous study.[8]

We have used a proteomic approach at the subcellular level to analyze the cytosolic, membrane/organelle, nuclear, and cytoskeletal subproteomes simultaneously in cells exposed to a fractionated 70% ethanolic extract of propolis, EL70. This has provided further insight into the molecular mechanisms behind propolis activity. Most of the changes at the proteome level investigated here were involved in carbohydrate and energy metabolism, actin filament dynamics, oxidative stress response, and protein folding.

AUTHOR INFORMATION

Corresponding Author

*Tel.: +386-1-3203729. Fax: +386-1-2574092. E-mail: polona.jamnik@bf.uni-lj.si.

Funding

This study was partly supported by the European Social Fund within the National Programme−Innovative scheme for funding doctoral programmes (278-246). No additional external funding was received for this study. The funders had no role in the study design, data collection and analysis, decision to publish, or preparation of the manuscript.

Notes

The authors declare no competing financial interest.

REFERENCES

(1) Burdock, G. A. Review of the biological properties and toxicity of bee propolis (propolis). *Food Chem. Toxicol.* **1998**, *36*, 347−363.

(2) Bueno-Silva, B.; Alencar, S. M.; Koo, H.; Ikegaki, M.; Silva, G. V.; Napimoga, M. H.; Rosalen, P. L. Anti-inflammatory and antimicrobial evaluation of neovestitol and vestitol isolated from Brazilian red propolis. *J. Agric. Food Chem.* **2013**, *61*, 4546−4550.

(3) Piccinelli, A. L.; Mencherini, T.; Celano, R.; Mouhoubi, Z.; Tamendjari, A.; Aquino, R. P.; Rastrelli, L. Chemical composition and antioxidant activity of Algerian propolis. *J. Agric. Food Chem.* **2013**, *61*, 5080−5088.

(4) Papotti, G.; Bertelli, D.; Bortolotti, L.; Plessi, M. Chemical and functional characterization of Italian propolis obtained by different harvesting methods. *J. Agric. Food Chem.* **2012**, *60*, 2852−2862.

(5) Kamiya, T.; Nishihara, H.; Hara, H.; Adachi, T. Ethanol extract of Brazilian red propolis induces apoptosis in human breast cancer MCF-7 cells through endoplasmic reticulum stress. *J. Agric. Food Chem.* **2012**, *60*, 11065−11070.

(6) Lotti, C.; Piccinelli, A. L.; Arevalo, C.; Ruiz, I.; Migliani De Castro, G. M.; Figueira Reis De Sá, L.; Tessis, A. C.; Ferreira-Pereira, A.; Rastrelli, L. Constituents of Hondurian propolis with inhibitory effects on Saccharomyces cerevisiae multidrug resistance protein Pdr5p. *J. Agric. Food Chem.* **2012**, *60*, 10540−10545.

(7) Cigut, T.; Polak, T.; Gašperlin, L.; Raspor, P.; Jamnik, P. Antioxidative activity of propolis extract in yeast cells. *J. Agric. Food Chem.* **2011**, *59*, 11449−11455.

(8) Petelinc, T.; Polak, T.; Demšar, L.; Jamnik, P. Fractionation of phenolic compounds extracted from propolis and their activity in the yeast *Saccharomyces cerevisiae*. *PLoS One* **2013**, *8*, e56104.

(9) Ma, D. Applications of yeast in drug discovery. *Prog. Drug Res.* **2001**, *57*, 117−162.

(10) Menacho-Marquez, M.; Murguia, J. R. Yeast on drugs: *Saccharomyces cerevisiae* as a tool for anticancer drug research. *Clin. Transl. Oncol.* **2007**, *9*, 221−228.

(11) Parsons, A. B.; Geyer, R.; Hughes, T. R.; Boone, C. Yeast genomics and proteomics in drug discovery and target validation. *Prog. Cell Cycle Res.* **2003**, *5*, 159−166.

(12) Foury, F. Human genetic diseases: A cross-talk between man and yeast. *Gene* **1997**, *195*, 1−10.

(13) Guthrie, C.; Fink, G. R. Guide to yeast genetics and molecular biology. *Methods Enzymol.* **1991**, *194*, 1−863.

(14) Sturgeon, C. M.; Kemmer, D.; Anderson, H. J.; Roberge, M. Yeast as a tool to uncover the cellular targets of drugs. *Biotechnol. J.* **2006**, *1*, 289−298.

(15) Cox, M. M.; Doudna, J.; O'Donnell, M. *Molecular Biology: Principles and Practice*; W. H. Freeman and Company: New York, 2012; p 809.

(16) Huber, L. A.; Pfaller, K.; Vietor, I. 2003. Organelle proteomics: Implications for subcellular fractionation in proteomics. *Circ. Res.* **2003**, *92*, 962−968.

(17) Rockstroh, M.; Müller, S. A.; Jende, C.; Kerzhner, A.; von Bergen, M.; Tomm, J. M. Cell fractionation - an important tool for compartment proteomics. *OMICS* **2011**, *1*, 135−143.

(18) Abdolzade-Bavil, A.; Hayes, S.; Goretzki, L.; Kröger, M.; Anders, J.; Hendriks, R. Convenient and versatile subcellular extraction procedure, that facilitates classical protein expression profiling and functional protein analysis. *Proteomics* **2004**, *4*, 1397−1405.

(19) Sawhney, S.; Stubbs, R.; Hood, K. Reproducibility, sensitivity and compatibility of the ProteoExtract subcellular fractionation kit with saturation labeling of laser microdissected tissues. *Proteomics* **2009**, *9*, 4087−4092.

(20) Murray, C. I.; Barrett, M.; Van Eyk, J. E. Assessment of ProteoExtract subcellular fractionation kit reveals limited and incomplete enrichment of nuclear subproteome from frozen liver and heart tissue. *Proteomics* **2009**, *9*, 3934−3938.

(21) Börner, A.; Warnken, U.; Schnölzer, M.; von Hagen, J.; Giese, N.; Bauer, A.; Hoheisel, J. Subcellular protein extraction from human pancreatic cancer tissues. *Biotechniques* **2009**, *46*, 297−304.

(22) Bradford, M. M. A rapid and sensitive method for the quantitation of microgram quantities of protein utilizing the principle of protein-dye binding. *Anal. Biochem.* **1976**, *72*, 248−254.

(23) Görg, A. Two-dimensional electrophoresis. *Nature* **1991**, *349*, 545−546.

(24) Ivancic, T.; Jamnik, P.; Stopar, D. Cold shock CspA and CspB protein production during periodic temperature cycling in *Escherichia coli*. *BMC Res. Notes* **2013**, *6*, 248.

(25) Wiederhold, E.; Veenhoff, L. M.; Poolman, B.; Slotboom, D. J. Proteomics of *Saccharomyces cerevisiae* organelles. *Mol. Cell. Proteomics* **2010**, *9*, 431−345.

(26) Gauthier, D. J.; Lazure, C. Complementary methods to assist subcellular fractionation in organellar proteomics. *Expert Rev. Proteomics* **2008**, *5*, 603−617.

(27) Butler, G. S.; Overall, C. M. Proteomic identification of multitasking proteins in unexpected locations complicates drug targeting. *Nat. Rev. Drug Discovery* **2009**, *8*, 935−948.

(28) Patton, W. F. Proteome analysis. II. Protein subcellular redistribution: Linking physiology to genomics via the proteome and separation technologies involved. *J. Chromatogr., B: Biomed. Sci. Appl.* **1999**, *722*, 203−223.

(29) Gruber, J. V.; Holtz, R. Examining the genomic influence of skin antioxidants in vitro. *Mediators Inflammation* **2010**, 230450-1−230450-10.

(30) de Castro, P. A.; Savoldi, M.; Bonatto, D.; Malavazi, I.; Goldman, M. H.; Berretta, A. A.; Goldman, G. H. Transcriptional profiling of *Saccharomyces cerevisiae* exposed to propolis. *BMC Complementary Altern. Med.* **2012**, *12*, 194-1−194-14.

(31) Barlak, Y.; Değer, O.; Colak, M.; Karatayl1, S. C.; Bozday1, A. M.; Yücesan, F. Effect of Turkish propolis extracts on proteome of prostate cancer cell line. *Proteome Sci.* **2011**, *9*, 74-1−74-11.

(32) Ralser, M.; Wamelink, M. M.; Kowald, A.; Gerisch, B.; Heeren, G.; Struys, E. A.; Klipp, E.; Jakobs, C.; Breitenbach, M.; Lehrach, H.; Krobitsch, S. Dynamic rerouting of the carbohydrate flux is key to counteracting oxidative stress. *J. Biol.* **2007**, *6*, 10-1−10-18.

(33) Ganguli, D.; Kumar, C.; Bachhawat, A. K. The alternative pathway of glutathione degradation is mediated by a novel protein complex involving three new genes in *Saccharomyces cerevisiae*. *Genetics* **2007**, *175*, 1137−1151.

(34) Kaur, H.; Kumar, C.; Junot, C.; Toledano, M. B.; Bachhawat, A. K. Dug1p Is a Cys-Gly peptidase of the gamma-glutamyl cycle of *Saccharomyces cerevisiae* and represents a novel family of Cys-Gly peptidases. *J. Biol. Chem.* **2009**, *284*, 14493−14502.

(35) Baudouin-Cornu, P.; Lagniel, G.; Kumar, C.; Huang, M. E.; Labarre, J. Glutathione degradation is a key determinant of glutathione homeostasis. *J. Biol. Chem.* **2012**, *287*, 4552−4561.

(36) Penninckx, M. J. An overview on glutathione in *Saccharomyces* versus non-conventional yeasts. *FEMS Yeast Res.* **2002**, *2*, 295−305.

(37) Odat, O.; Matta, S.; Khalil, H.; Kampranis, S. C.; Pfau, R.; Tsichlis, P. N.; Makris, A. M. Old yellow enzymes, highly homologous FMN oxidoreductases with modulating roles in oxidative stress and programmed cell death in yeast. *J. Biol. Chem.* **2007**, *282*, 36010−36023.

(38) Mullins, R. D.; Hauser, J. A.; Pollard, T. D. The interaction of Arp2/3 complex with actin nucleation, high affinity pointed end capping, and formation of branching networks of filaments. *Proc. Natl. Acad. Sci. U.S.A.* **1998**, *95*, 6181−6186.

(39) Schindler, R.; Weichselsdorfer, E.; Wagner, O.; Bereiter-Hahn, J. Aldolase-localization in cultured cells: Cell-type and substrate-specific regulation of cytoskeletal associations. *Biochem. Cell Biol.* **2001**, *79*, 719−728.

(40) Mounier, N.; Arrigo, A. P. Actin cytoskeleton and small heat shock proteins: How do they interact? *Cell Stress Chaperones* **2002**, *7*, 167−176.

(41) Guay, J.; Lambert, H.; Gingras-Breton, G.; Lavoie, J. N.; Huot, J.; Landry, J. Regulation of actin filament dynamics by p38 map kinase-mediated phosphorylation of heat shock protein 27. *J. Cell Sci.* **1997**, *110*, 357−368.

(42) Jakob, U.; Gaestel, M.; Engel, K.; Buchner, J. Small heat shock proteins are molecular chaperones. *J. Biol. Chem.* **1993**, *268*, 1517−1520.
(43) Dalle-Donne, I.; Rossi, R.; Milzani, A.; Di Simplicio, P.; Colombo, R. The actin cytoskeleton response to oxidants: From small heat shock protein phosphorylation to changes in the redox state of actin itself. *Free Radical Biol. Med.* **2001**, *31*, 1624−1632.
(44) Feldman, R. I.; Bernstein, M.; Schekman, R. Product of SEC53 is required for folding and glycosylation of secretory proteins in the lumen of the yeast endoplasmic reticulum. *J. Biol. Chem.* **1987**, *262*, 9332−9339.
(45) Sanderson, H. S.; Clarke, P. R. Cell biology: Ran, mitosis and the cancer connection. *Curr. Biol.* **2006**, *16*, R466−R468.
(46) Xia, F.; Lee, C. W.; Altieri, D. C. Tumor cell dependence on Ran-GTP-directed mitosis. *Cancer Res.* **2008**, *68*, 1826−1833.
(47) Lui, K.; Huang, Y. RanGTPase: A key regulator of nucleocytoplasmic trafficking. *Mol. Cell. Pharmacol.* **2009**, *1*, 148−156.